Development 123, 275-283
Printed in Great Britain © The Company of Biologists Limited 1996
DEV3384

Mutations affecting development of the zebrafish ear

Jarema Malicki[¶], Alexander F. Schier, Lilianna Solnica-Krezel, Derek L. Stemple, Stephan C. F. Neuhauss, Didier Y. R. Stainier*, Salim Abdelilah, Zehava Rangini[†], Fried Zwartkruis[‡] and Wolfgang Driever[§]

Cardiovascular Research Center, Massachusetts General Hospital and Harvard Medical School, 13th Street, Building 149, Charlestown, MA 02129, USA

*Present address: School of Medicine, Department of Biochemistry and Biophysics, UCSF, San Francisco, CA 94143-0554, USA
[†]Present address: Department of Oncology, Sharett Institute, Hadassah Hospital, Jerusalem 91120, Israel
[‡]Present address: Laboratory for Physiological Chemistry, Utrecht University, Universiteitsweg 100, 3584 CG Utrecht, The Netherlands
[¶]Present address: Harvard Medical School and MEEI, Department of Ophthalmology, 243 Charles Street, Boston, MA 02114, USA
[§]Author for correspondence (e-mail: driever@helix.mgh.harvard.edu)

SUMMARY

In a large scale screen for genetic defects in zebrafish embryogenesis we identified mutations affecting several aspects of ear development, including: specification of the otic placode, growth of the otic vesicle (otocyst), otolith formation, morphogenesis of the semicircular canals and differentiation of the otic capsule. Here we report initial phenotypic and genetic characterization of 20 of these mutations defining 13 independent loci. Embryos mutant at the *quadro* locus display abnormal specification of the otic placode. As revealed by *dlx-3* expression, the otic field in the mutant embryos is smaller or split into two fields. At later stages of development the ear of *quadro* mutants is frequently divided into two smaller, incomplete units. Four loci affect ear shape shortly after formation of the otic vesicle. All of them also display abnormal brain morphology. Mutations in five loci result in the absence of otolith formation; two of these also produce changes of ear morphology. Two loci, *little richard* and *golas*, affect morphology of the otic vesicle shortly before formation of the semicircular canals. In both cases the morphogenesis of the semicircular canals is disrupted. Finally, the *antytalent* locus is involved in late expansion of the ear structure. Analysis of mutations presented here will strengthen our understanding of vertebrate ear morphogenesis and provide novel entry points to its genetic analysis.

Key words: ear, patterning, zebrafish, *quadro*, *little richard*, *golas*, *antytalent*

INTRODUCTION

The vertebrate inner ear has two major functions: it is responsible for the maintenance of body balance and for auditory perception. The morphological form of the inner ear is relatively similar in all groups of jawed vertebrates (Retzius, 1881, 1884). It consists of three chambers of varying prominence, the utriculus, sacculus and lagena and three semicircular canals. The semicircular canals both begin and end in the utriculus and each is located in a separate plane, at right angles to the other two. A spherical widening, known as the ampulla, is located at one end of each semicircular canal. The walls of the inner ear are lined with epithelium which contains specialized sensory areas. These regions contain a mechanoreceptive cell type known as the hair cell. Three large and five smaller sensory areas are present in the ear of the adult zebrafish (Platt, 1993). A large sensory area, called the macula is localized in each of the ear chambers in bony fishes, forming the support for a largely inorganic aggregation of calcium salts, termed the otolith (Lim, 1980). Three smaller sensory areas (cristae) are located in the ampulae of the semicircular canals.

The sensory epithelia of the inner ear chambers respond to movements of otoliths providing information about tilt and linear acceleration, while the cristae of the semicircular canals provide information about turning movements (Hawkins and Horner, 1981). In addition to serving the role of a balance organ, the maculae of the cyprinid fishes are most likely also involved in hearing (Popper and Fay, 1993). In zebrafish and other cyprinids, the sound induced vibrations of the swim bladder are thought to be conveyed to the ear chambers by a chain of specialized bones, named Weberian ossicles (Chranilov, 1927; reviewed by Popper and Fay, 1993). In higher vertebrates the function of hearing is fulfilled by the cochlea, a structure homologous to the lagena.

Development of a structure as complex as the vertebrate inner ear undoubtedly requires an intricate network of genetic interactions. Several genes characterized at the molecular level are known to be involved in the development of the mammalian ear (reviewed by Steel and Brown, 1994). Genetic lesions in *Pax-3*, *Int-2* and *Hoxa-1* have been shown to produce inner ear defects (Epstein et al., 1991; Chisaka et al., 1992; Mansour et al., 1993). A large group of loci involved in the development of the mouse inner ear were isolated on the basis of behavioral abnormalities. Mutations in these loci produce a behavioral disorder known as the waltzing syndrome which involves hyperactivity, tendency to run in circles and jerking movements of the head. The ear defects of these mutants frequently involve malformations of the inner ear chambers and the semicircular canals (Deol, 1968, 1980). The *kreisler (kr)*

phenotype is one of the most severe in this group and in extreme cases leads to the complete absence of any recognizable inner ear elements (Deol, 1964). Positional cloning of the *kreisler* locus has recently revealed that it encodes a transcription factor expressed in rhombomeres 5 and 6 of the hindbrain (Cordes and Barsh, 1994).

The development of the zebrafish ear has been described in detail (Waterman and Bell, 1984; Haddon and Lewis, 1996). The first morphological manifestation of the ear is a condensation of ectodermal cells known as the otic placode. The otic placodes first become visible around the 14 somite stage and are located on both sides of the hindbrain approximately midway between the eye and the first somite. Cells in the initially solid mass of the otic placode rearrange, forming the lumen of the otic vesicle. Two otoliths appear in the otic vesicle at approximately 19 hpf (hours postfertilization). Between 19 and 44 hpf the otic vesicle increases in size and the otoliths become larger (Fig. 1A). A series of morphological changes which lead to the formation of semicircular canals is initiated at 44 hpf with the appearance of finger-like protrusions growing into the cavity of the otic vesicle (Fig. 1B; Waterman and Bell, 1984). Protrusions growing from the opposite walls of the otocyst fuse together, forming three columns of tissue which delimit the space of individual semicircular canals. The anterior semicircular canal is the first to be formed and the lateral is the last. The process of semicircular canal formation is completed by 64 hpf (Waterman and Bell, 1984). The subdivision of the zebrafish ear into utriculus, sacculus and lagena is a relatively late event. The three chambers are not distinct at 5 days postfertilization (dpf) (Fig. 1C).

In a large mutagenesis screen in zebrafish we searched for recessive, zygotic loci involved in ear morphogenesis during the first 5 days of development. We identified mutations affecting several aspects of development: specification of the otic placode; growth of the otic vesicle; otolith formation; morphogenesis of the semicircular canals and late expansion of the ear structure. Here, we report initial genetic and phenotypic characterization of 20 mutations affecting early ear development.

MATERIALS AND METHODS

Genetic analysis

Mutations were induced using N-ethyl-N-nitrosourea (ENU) as described previously (Solnica-Krezel et al., 1994). All mutants were initially identified in the progeny of crosses between individuals of the F_2 generation bred from the mutagenized G_0 males (Driever et al., 1996). All crosses that led to the identification of mutant phenotypes were repeated. For further analysis, heterozygous carriers of mutant alleles were outcrossed to wild-type AB (Chakrabarti et al., 1983), Tübingen (Mullins et al., 1994) or India (Knapik et al., 1996) strains. Mutant heterozygotes were identified in the progeny of outcrosses by sibling mating.

Complementation tests were performed between heterozygous carriers of mutations falling into the same phenotypic category. At least 30 embryos, often from two independent crosses were scored for the mutant phenotype. Complementation testing was not performed for *m219*.

Phenotypic analysis

Embryos were maintained at 28°C in egg water (Westerfield, 1994) with the addition of methylene blue (Sigma, Inc.) at a concentration of 1 mg/l. Staging was performed as described previously (Kimmel et al., 1995). For observations, embryos were anesthetized with a 0.02% solution of 3-aminobenzoic acid methyl ester (Sigma, Inc.) and embedded in 3% methylcellulose in egg water. Living embryos were initially observed and photographed under a dissecting microscope. Detailed observations were conducted using an Axiophot microscope and Nomarski optics (Zeiss, Inc.).

In situ hybridization was performed with digoxigenin-labeled probes on whole embryos as described previously (Oxtoby and Jowett, 1993). Expression patterns were photographed in embryos mounted in 3% methyl cellulose.

RESULTS

As a part of a large scale mutagenesis screen we searched for mutations affecting development of the zebrafish ear (Driever et al., 1996). The ear of the zebrafish embryo is relatively large and easily accessible to visual inspection (Fig. 1). Fig. 1D shows a schematic representation of morphological elements

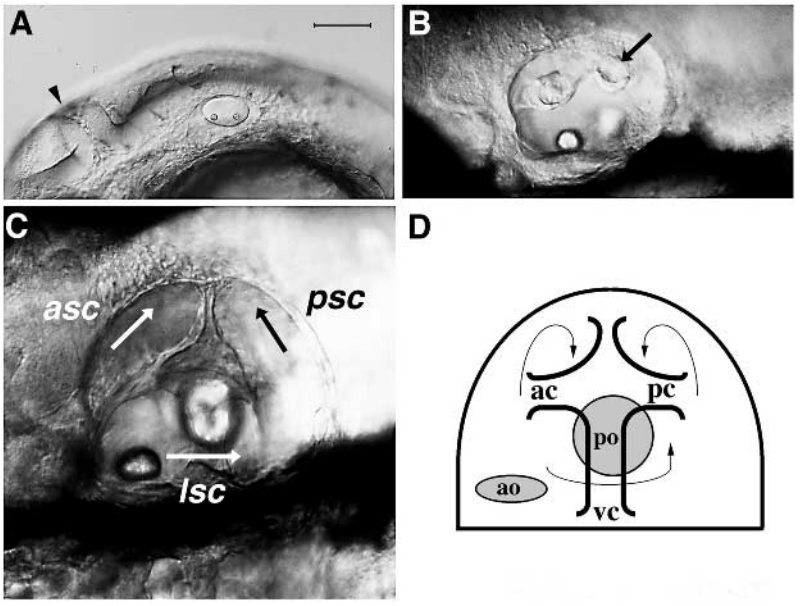

Fig. 1. Ear development in wild-type zebrafish. (A) At 30 hpf the zebrafish ear is an epithelial vesicle containing two otoliths. (Arrowhead indicates the midbrain-hindbrain boundary.) (B) Appearance of the zebrafish ear at approximately 60 hpf. Development of the semicircular canals is initiated by the appearance of epithelial protrusions (arrow) extending into the lumen of the otocyst. Protrusions growing from opposing walls of the otocyst fuse together forming columns surrounded by the lumen of semicircular canals. Formation of columns delimiting the anterior and posterior semicircular canals is well advanced at this stage. (C) At 5 dpf the semicircular canals are well formed and easily recognizable in a living embryo (arrows). (D) A schematic representation of the major morphological elements of the zebrafish ear accessible to visual inspection at 5 dpf (compare with photograph in C). The anterior (ac), posterior (pc) and ventral (vc) columns delimit the lumen of semicircular canals (arrows). The posterior otolith (po) is located behind the translucent, ventral column. ao, anterior otolith; asc, anterior semicircular canal; psc, posterior semicircular canal; lsc, lateral semicircular canal. Scale bar, 100 μm.

which are easily recognizable in the zebrafish ear at 5 dpf (compare with the photograph in 1C). The shape of semicircular canals is easy to follow at this stage in both lateral and dorsal views. In the course of screening, several aspects of ear development, including size and shape of the otic vesicle, presence and positioning of otoliths, morphology of the semicircular canals and the otic capsule were evaluated at 1, 2, 3 and 5 dpf.

Some aspects of ear development were not accessible to inspection during our screen. For example, we were unable to monitor abnormalities in the positioning of cristae. Likewise, we did not screen for defects in developmental events taking place after 5 dpf, such as formation of the lagena and its otolith.

Not all phenotypes affecting the ear were subject to further analysis. Numerous mutations resulting in a general delay of development frequently led to a somewhat reduced ear size at day 2 and did not form semicircular canals. Mutations affecting formation of cartilage also frequently involved abnormal morphogenesis of semicircular canals (Neuhauss et al., 1996).

Phenotypic characterization of the isolated mutations allowed us to divide them into five categories, each affecting different aspects of ear development: (1) abnormal specification of the otic placode; (2) defective early morphogenesis of the otic vesicle; (3) absence of otoliths; (4) aberrant late morphogenesis of the otic vesicle; (5) defective late expansion of the ear structure. Below we present a phenotypic analysis of mutants belonging to each of the above categories.

Specification of the otic placode

The mutation *quadro (quo)*^{m271} affects ear development at the earliest stages of otic placode formation. The otic placodes of *quo*^{m271} are frequently smaller or split into two fields. The phenotype of this mutant is variable and asymmetrical. In some individuals the otic vesicle is reduced in size, in others two incomplete otocysts are formed. Otoliths frequently develop in each of the incomplete otocysts (Fig. 2A,B). The epithelial protrusions associated with formation of semicircular canals initially form but do not reach their mature shape (arrowheads in Fig. 2B). The ear phenotype of *quo*^{m271} is not fully penetrant. In a cross between two heterozygous animals approximately 15% (29/190) of progeny develop ear abnormalities at 1 dpf.

Specification of the ear rudiment is detectable by expression of the *dlx-3* gene before the morphological appearance of the otic placode (Ekker et al., 1992). To investigate whether *quo*^{m271} affects specification of the otic placode, we analyzed *dlx-3* expression by in situ hybridization at the 10 somite stage (14 hpf). At this stage *dlx-3* is expressed in two ellipsoid patches of cells located symmetrically one on each side of the wild-type hindbrain (arrowhead in Fig. 2C). The *dlx-3* expression domain is split into two parts in a fraction of embryos originating from a cross between two *quo*^{m271} heterozygotes (arrowheads in Fig. 2D). Such expression pattern is never seen in the progeny of wild-type individuals and indicates that the ear patterning defect in *quo*^{m271} mutants is present at the onset of the otic placode formation.

The ear defect of *quo*^{m271} mutants is also evident in the expression pattern of *msx-C*. In the wild type at 60 hpf *msx-C* is expressed in three distinct patches in the ventral portion of the otic vesicle (Ekker et al., 1992; arrows in Fig. 2E). In *quo*^{m271} mutants, the *msx-C* expression domains are frequently fused or missing (Fig. 2F). In order to assess whether the ear

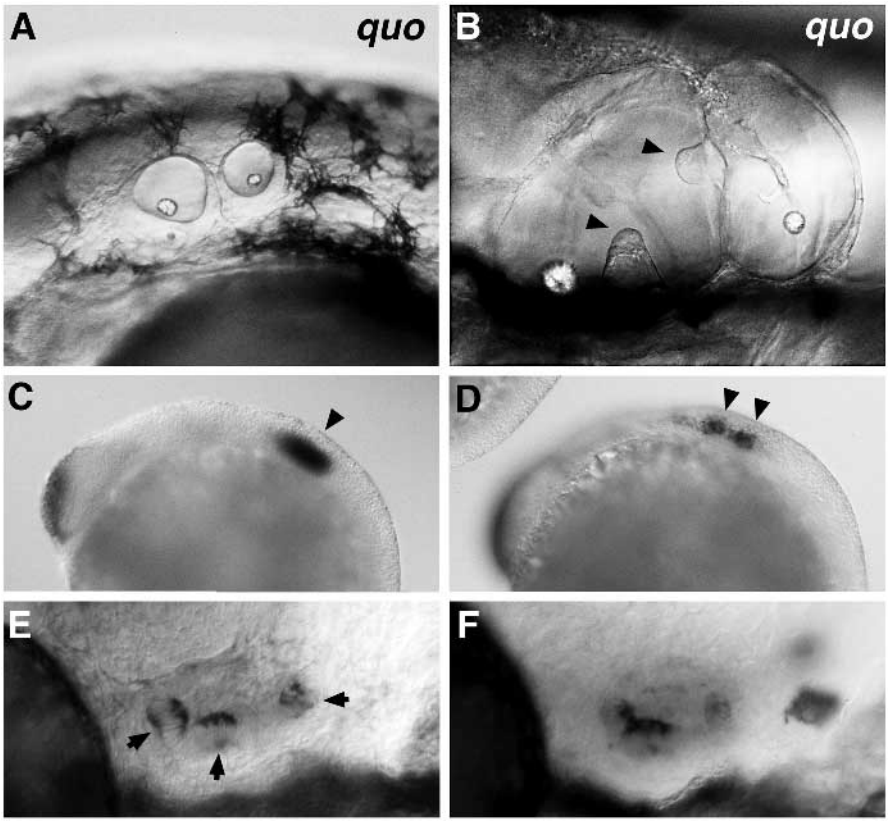

Fig. 2. The ear phenotype of *quadro (quo)*^{m271} mutants. In some mutant embryos the otocyst is split into two incomplete vesicles. A and B show the appearance of ears in the mutant at 36 hpf and 5 dpf respectively. Epithelial protrusions form but frequently do not develop into columns (arrowheads in B). At 14 hpf *dlx-3* is expressed in the forming otic placode of wild-type embryos (arrowhead in C). In some mutant embryos, the *dlx-3* expression domain is split into two smaller fields at this stage (arrowheads in D). In the wild-type ear the *msx-C* gene is expressed in three distinct patches at 60 hpf (arrows in E). The *msx-C* expression domains are frequently fused or absent in *quo*^{m271} embryos at this stage (F). In all panels anterior is left and dorsal up.

Table 1. Mutations affecting development of the zebrafish ear

Locus name	Alleles	Ear phenotype	Other phenotypes	Ref.
Group I: Specification of the otic placode				
quadro (quo)	*m271*	Ov. split (1 dpf), scc. abnormal, ot. mispositioned	Branchial arches	a
Group II: Early morphogenesis of the otic vesicle				
snakehead (snk)	*m115, m273, m523*	Ov. narrow and elongated, scc. not formed, ot. very small	Brain, heart, circulation, touch response	b
mind bomb (mib)	*m132, m178*	Ov. smaller and abnormal shape, scc. abnormal, ot. small or missing	Brain, circulation, pigmentation, touch response	b
pandora (pan)	*m313*	Ov. smaller and abnormal shape, scc. not formed, ot. small or missing	Brain, eye, heart, circulation, pigmentation, tail, touch response	c, d, e
flachland (fll)	*m517*	Ov. smaller, frequently one ot.	Brain shape, circulation	b
Group III: Otolith formation				
empty ear (emp)	*m107*	Ot. missing		
–	*m219*	Ot. missing		
straight edge (sed)	*m327*	Ot. small or missing		
helter skelter (hek)	*m504*	Ov. expanded, ot. missing		
znikam (znk)	*m574*	Ov. retarded (3 dpf), ot. missing		
haos (hos)	*m751*	Ot. mispositioned, smaller or missing		
Group IV: Late morphogenesis of the otic vesicle				
little richard (lit)	*m181, m433*	Ov. reduced (2 dpf), scc. not formed, ot. small and close together	Branchial arches, posterior head, circulation	a
golas (gos)	*m241, m618*	Ov. reduced (2 dpf), scc. abnormal, ot. small and close together	Pigmentation	
Group V: Late expansion of the ear structure				
antytalent (ant)	*m317 , m426*	Ov. reduced (3 dpf)		

Other phenotypic aspects of mutants presented in this table are described by: a, Neuhauss et al. (1996); b, Schier et al. (1996); c, Abdelilah et al. (1996); d, Stainier et al. (1996); e, Malicki et al. (1996). Mutations without locus name were not complemented. ot, otoliths; ov, otic vesicle; scc, semicircular canals; dpf, days postfertilization.

phenotype of *quo*^{m271} is associated with a hindbrain patterning defect, we performed in situ hybridization with the *krox-20* probe on 10 somite stage embryos. In wild-type embryos the *krox-20* gene is expressed in two distinct domains which correspond to rhombomeres 3 and 5 (Oxtoby and Jowett, 1993). We did not detect any obvious differences between the expression pattern of *krox-20* in wild-type and *quo*^{m271}animals at this stage (not shown).

Early morphogenesis of the otic vesicle

Seven mutations in four loci were found to affect early development of the otocyst (Table 1, Fig. 3). The abnormal shape

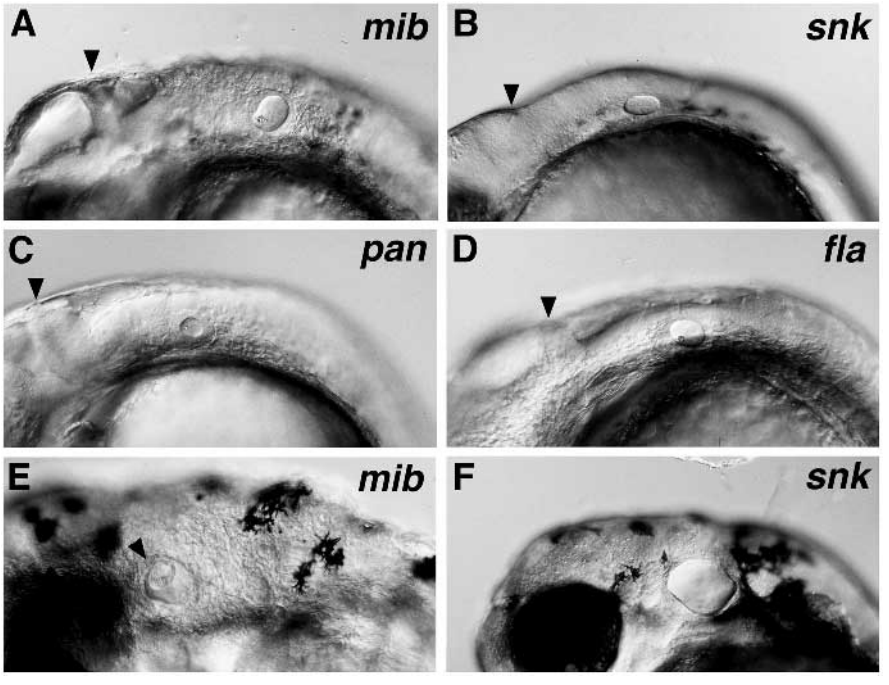

Fig. 3. Phenotypes resulting from mutations affecting early morphogenesis of the otic vesicle. At 30 hpf the otic vesicles of (A) *mind bomb (mib)*^{m178}; (B) *snakehead (snk)*^{m273}; (C) *pandora (pan)*^{m313}; and (D) *flachland (fll)*^{m517} mutants are of abnormal size and shape (compare with the wild type in Fig. 1A). Formation of otoliths is also affected in these mutants. Epithelial protrusions form in the otic vesicle of *mib*^{m178} at 60 hpf (arrowhead in E). At 60 hpf the otic vesicle of *snk*^{m273} frequently does not form protrusions and appears to be disproportionately large compared to other organs (F). Arrowheads in A-D indicate the midbrain-hindbrain boundary. In all panels anterior is left and dorsal up.

of the otic vesicle is detectable in these mutants by 24 hpf. The wild-type otic vesicle is ellipsoid at 30 hpf and its long axis is parallel to the anteroposterior body axis (Fig. 1A). In contrast, the otic vesicles of *mind bomb (mib)*^{m178}, *pandora (pan)*^{m313}, and *flachland (fll)*^{m517} are frequently smaller and more round (Fig. 3A,C,D). The otocyst of *snakehead (snk)*^{m273} is narrower in its dorsoventral dimension than its wild-type counterpart (Fig. 3B). All four loci affect development of the otoliths. The otoliths of *snk*^{m273} are barely visible. In *mib*^{m178} and *pan*^{m313} the otoliths are often missing or only one otolith can be found. Frequently only one otolith is present in *fll*^{m517}.

Defects of the semicircular canals are variable among mutants in this group. This aspect of ear development is most severely affected in *pan*^{m313} and *snk*^{m273} which rarely initiate formation of the semicircular canals. The otic vesicle of *snk*^{m273} appears abnormally large relative to other organs at 2 dpf (Fig. 3F). In *mib*^{m178} protrusions form in the otic vesicles but these do not develop the normal pattern of columns (arrowhead in Fig. 3E). Their presence suggests that the reduced ear size in this mutant is not simply due to a developmental arrest. The semicircular canals are relatively unaffected in *fll*^{m517} and develop normally in at least some mutant animals (not shown). In order to investigate by additional means whether the patterning of the otic vesicle in *fll*^{m517} is normal, we performed in situ hybridization with the *msx-C* probe on the mutant embryos at 60 hpf. The *msx-C* expression pattern in *fll*^{m517} is indistinguishable from wild-type pattern at this stage (not shown).

The brain morphology of mutants in this category is abnormal. The midbrain ventricle appears to be abnormally large in *mib*^{m178}. The *mib* locus is associated with a particularly intriguing phenotype; supernumerary primary neurons are generated in the *mib* mutants (Schier et al., 1996). The remaining mutations result in a reduction in the size of the brain ventricles, which is most pronounced in *snakehead* (Schier et al., 1996).

Otolith formation

Six mutations isolated in our screen result in a lack of otolith formation (Table 1; Fig. 4). In *empty ear (emp)*^{m107}, *straight edge (sed)*^{m327}, *haos (hos)*^{m751} and *m219* the gross morphology of the otic vesicles and later of the semicircular canals is normal (Fig. 4A,E). In contrast, *helter skelter(hek)*^{m504} and *znikam(znk)*^{m574} produce changes in ear morphology. At 36 hpf the otocyst of *hek*^{m504} animals is larger than its wild-type counterpart (Fig. 4C compare with B). In some *hek*^{m504} mutant animals the positioning of the protrusions forming the semicircular canals appears to be slightly abnormal at 2 dpf (not shown). The abnormalities of the semicircular canals are no longer apparent at 5 dpf. The morphological defect in *znk*^{m574} becomes most obvious around 72 hpf and has varying prominence. In the most affected mutant animals the otic capsule and the semicircular canals are barely visible at this stage. In the least affected individuals, the ear morphology is fairly normal. Fig. 4D shows a moderately severe form of this phenotype at 3 dpf. The overall size of the ear is reduced and the columns delimiting the semicircular canals are not as distinct as in the wild type. Interestingly, these morphological abnormalities are no longer obvious by 5 dpf.

The absence of otoliths is not fully penetrant in *sed*^{m327}, *hos*^{m751} *and znk*^{m574}. In some *sed*^{m327} and *znk*^{m574} mutant animals a single, small otolith is present in one of the normal positions. In some outcrosses, *hos*^{m751} mutants develop supernumerary, mispositioned otoliths (arrowheads in Fig. 4E). At 60 hpf the expression pattern of *msx-C* in *znk*^{m574} appears to be somewhat abnormal. The two anterior expression domains are positioned closer to each other than in the wild type (not shown). In *emp*^{m107}, *hek*^{m504} and *hos*^{m751} the *msx-C* expression closely resembles the wild-type pattern (not shown).

Late morphogenesis of the otic vesicle

Two loci affect otic vesicle morphogenesis at later stages of development than the group II mutations (Table 1; Fig. 5). The *little richard* (*lit*) phenotype is first distinguishable shortly before the onset of semicircular canal formation. Of the two alleles recovered for this locus, *lit*^{m433} produces a stronger phenotype (Fig. 5B, compare with A). During late day 2 of

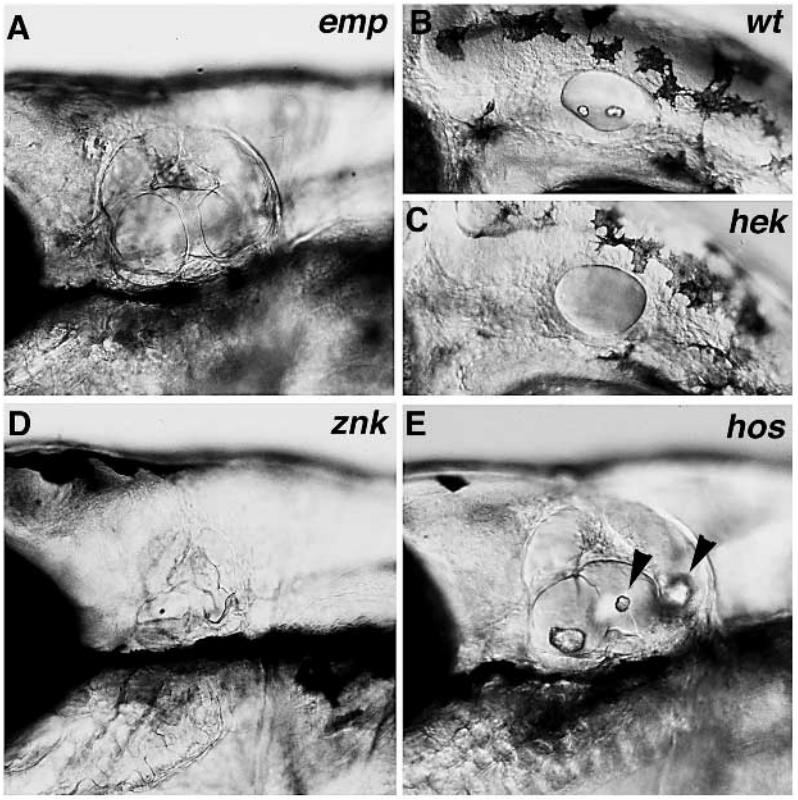

Fig. 4. Phenotypes involving absence of otoliths. (A) The morphology of semicircular canals is normal in *empty ear (emp)*^{m107} but the otoliths do not form. At 36 hpf the otic vesicle of *helter skelter (hek)*^{m504} larvae (C) appears to be larger than its wild-type counterpart (B). The ear of *znikam (znk)*^{m574} is smaller at 3 dpf than its wild-type equivalent and the otic capsule less distinct (D, compare with Fig. 5D). In some outcrosses ectopic otoliths form in the ears of *haos (hos)*^{m751} animals (arrowheads in E). In all panels anterior is left and dorsal up. A and E show larval ears at 5 dpf.

development, growth of the otic vesicle in *lit*^{m433} becomes slower and the formation of semicircular canals is not initiated. At 3 dpf the ear of these mutants is very small and undifferentiated in comparison to the wild type (Fig. 5B,E - compare with A,D). Two small otoliths are positioned next to each other. The reduced size of the otic vesicle is accompanied by an overall shortening of the posterior head region. The distance between the pectoral fin (arrowheads in Fig. 5A,B) and the eye is reduced in the mutant. The *msx-C* expression at 60 hpf is absent (Fig. 5H, compare with G). Lack of *msx-C* expression and absence of epithelial protrusions suggest that late patterning events are not initiated in the otic vesicle of *lit*^{m433} embryos.

The *golas (gos)* mutant embryos combine defective ear morphology and abnormal pattern of pigment cells. Two alleles are available at this locus: *gos*^{m241} and *gos*^{m618}. *gos*^{m618} is stronger and its phenotype is first detectable around 36 hpf. The epithelial protrusions start developing in these mutants but have abnormal shape and fail to form mature columns. At 3 dpf the otic capsule of *gos*^{m241} is slightly smaller than that of the wild type (Fig. 5A,C). The ear reduction is much stronger in *gos*^{m618} (Fig. 5F, compare with the wild type in D). In the most extreme cases the otic capsule surrounding two small otoliths is barely visible (not shown). Melanocytes are not observed in *gos*^{m618} and are restricted to the dorsal midline in *gos*^{m241}.

Late expansion of the ear structure

The two alleles isolated at the *antytalent (ant)* locus affect expansion of the ear (Table 1; Fig. 6). *ant*^{m426} appears to produce a somewhat stronger phenotype than *ant*^{m317}. Both alleles cause a slight reduction of ear size during day 4 of development. The semicircular canals and otoliths appear to have normal positioning and morphology at this stage. At 5 dpf the otic capsule and the semicircular canals of the mutant embryos are reduced and not easily recognizable in the lateral view (Fig. 6A; compare with the wild type in Fig. 1C). Also in the dorsal view, the otic capsule is flattened as compared to the wild type (Fig. 6C, compare with B). Two normal size otoliths persist at least until 5 dpf.

Other defects of ear development

A number of ear mutations isolated in our screen have not been analyzed here. These mutations fall into four subgroups. 13 mutations result in the presence of only one otolith (*m96*, *m150*, *m198*, *m234*, *m269*, *m392*, *m490*, *m539*, *m548*, *m554*, *m675*, *m690*, *m720*). Limited complementation analysis within this category revealed that at least five of them*: m150*, *m198*, *m234*, *m269* and *m392* affect the same locus. The second subgroup includes mutations resulting in a reduction of otolith size (*m251*, *m389*, *m428*, *m431*). A group of 4 mutations (*m286*, *m288*, *m293*, *m300*) affect otolith size as well as eye size and pigmentation (Malicki et al., 1996). The fourth group of 17 mutations lead to abnormal growth and differentiation of cartilage (Neuhauss et al., 1996). These mutations also affect development of epithelial protrusions in the otocyst and consequently formation of the semicircular canals.

DISCUSSION

Here we report identification of 20 mutations in 13 loci affecting several consecutive stages of ear development. The earliest phenotype, produced by a mutation in the locus *quadro* affects the very first step of ear morphogenesis – formation of the otic placode. In contrast, the latest onset phenotype – lack of ear expansion in the *antytalent* mutants – becomes apparent only after formation of the semicircular canals. The phenotypes of other mutants become noticeable at the intermediate stages and affect shaping of the otocyst, otolith formation and morphogenesis of the semicircular canals. The phenotypes of

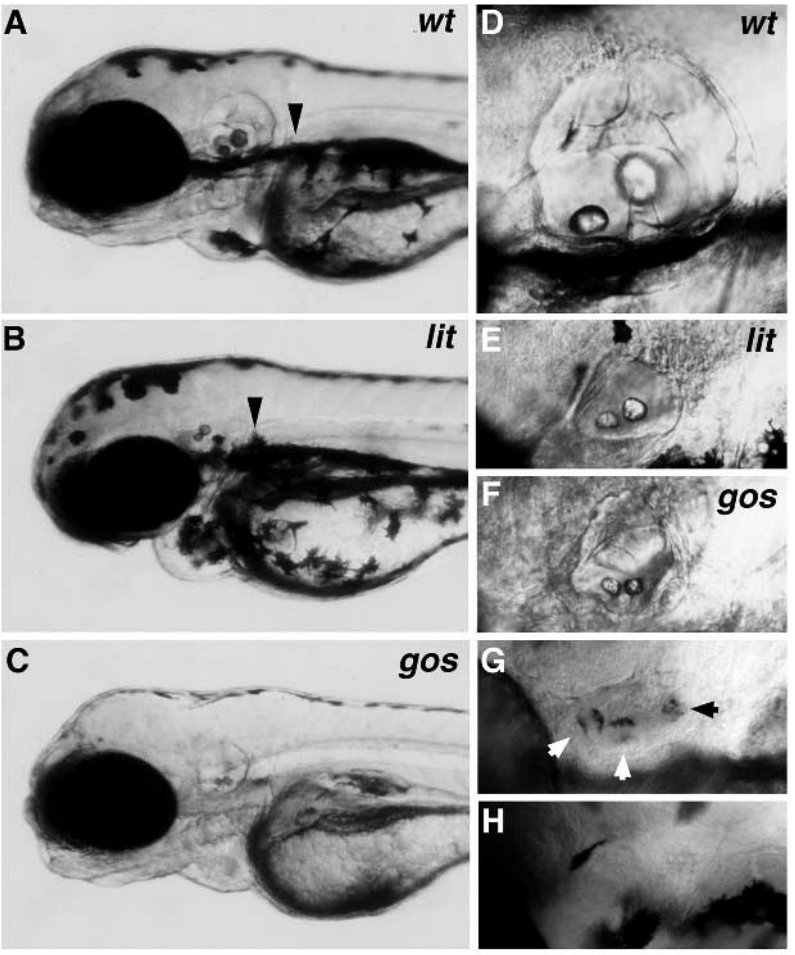

Fig. 5. The phenotypes of *little richard (lit)* and *golas (gos)* mutants. At 3 dpf the ear of *lit*^{m433} (B,E) is markedly smaller than its wild-type counterpart (A,D). In the wild-type larva the semicircular canals are well developed at this stage (D). In contrast, formation of semicircular canals in *lit*^{m433} mutants is not initiated (E). At 3 dpf the ear of *gos*^{m241} is smaller than its wild-type counterpart and has abnormal shape (C, compare with A). The *gos*^{m618} mutation produces a much more pronounced reduction of ear size (F, compare with the wild type in D). (G) Wild-type expression of *msx-C* at 60 hpf (arrows). (H) *msx-C* is not expressed in *lit*^{m433} at 60 hpf. Arrowheads in A and B indicate positioning of the pectoral fin. In all panels anterior is left and dorsal up.

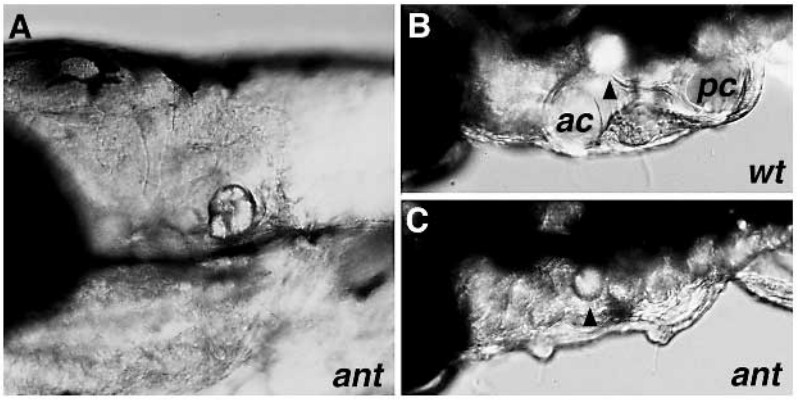

Fig. 6. The phenotype of *antytalent (ant)*^{m426} mutants at 5 dpf. (A) In the lateral view, the mutant otic capsule and semicircular canals are not easily recognizable at this stage. (B) In the dorsal view the anterior and posterior semicircular canals are clearly visible in the wild type. In contrast, the ear of *ant*^{m426} mutants (C) is flattened and the semicircular canals are not distinct. The arrowheads in B and C indicate positioning of the otolith. In A dorsal is up. In all panels anterior is left. ac, anterior canal; pc, posterior canal.

quadro and *antytalent* mutants appear to be opposites in yet another way: *antytalent* mutations affect growth of the ear but not its pattern, while *quo*^{m271} results in abnormal patterning of a normally sized ear. In many other mutants the ear patterning defects are accompanied by a reduction of ear size.

Early embryological experiments suggested that pattern formation in the developing ear depends on continued interaction of the otic vesicle with the hindbrain. In amphibian embryos, surgical replacement of the hindbrain with midbrain or spinal cord tissues results in the abnormal development of the otocyst which frequently does not form semicircular canals (Detwiler and Van Dyke, 1950, 1951). A close association of otic vesicle morphogenesis with brain development is also suggested by mouse mutants. In *kreisler* embryos the morphological appearance of rhombomeres is abnormal and the expression patterns of *Hoxb-1*; *Krox-20* and *Fgf-3* do not obey their wild-type expression boundaries in the hindbrain (Frohman et al., 1993). The developing otic vesicle is shifted to a more lateral location, the inner ear chambers, semicircular canals and the endolymphatic duct do not develop properly (Deol, 1964). The *kreisler* gene is expressed in the hindbrain but not in the otic vesicle suggesting that ear abnormalities in this mutant are secondary to the neural tube defect (Cordes and Barsh, 1994). Likewise, in *Hoxa-1* knockout mice abnormal hindbrain morphology is associated with malformations of the inner ear compartments and the endolymphatic duct (Chisaka et al., 1992).

Several mutations isolated in our screen involve both ear and brain defects. This association may reflect disruption of proper signaling events between the brain and the developing ear. Alternatively, the affected loci may function independently in the neural tube and the otic vesicle. Brain patterning was analyzed using molecular markers in two of the Group II mutants (Table 1) (Schier et al., 1996). The expression patterns of *krox-20* and *pax-2* in *fll*^{m517} and *rtk-1* in *snk*^{m273} do not display any obvious abnormalities.

The association of a strong ear patterning defect with a loss of pigmentation in *golas* is intriguing. Apart from these two abnormalities the *golas* mutants closely resemble the wild type. The pigmentation phenotype suggests a neural crest defect. One possible explanation for the association of these two phenotypes could be that mutations in the *golas* locus result in the absence of the neural crest-derived cells necessary for normal ear morphogenesis. Fate mapping experiments conducted in quail-chick chimeras indicate that neural crest-derived cells contribute to the formation of the otic capsule (Le Lievre, 1978; Noden, 1983). Their role in inner ear morphogenesis is, however, not clear. Neural crest ablation experiments conducted in medaka (*Oryzias latipes*) did not result in any obvious abnormalities of ear development (Langille and Hall, 1988). Mouse pigmentation mutants frequently display hearing abnormalities but do not have defects in early ear morphogenesis (Deol, 1970, 1980). In the mouse, the neural crest-derived melanoblasts and melanocytes are found in the vicinity of the developing ear. Their absence in the mutant *piebald lethal* (*s*^{l}) is not associated with gross defects of ear morphogenesis (Pavan and Tilghman, 1994).

The expression patterns of *Pax-2* and *dlx-3* suggest that the otic placode of the zebrafish embryo is specified by 11-12 hours of development (Krauss et al., 1991; Ekker et al., 1992). The *dlx-3* expression in *quadro*^{m271} indicates that the ear defect in this mutant is already present by 14 hpf. It is interesting that *quadro*^{m271} also affects development of the branchial arches. In the cephalic region of the zebrafish neural keel, neural crest migration is initiated at 15-16 hpf (Schilling and Kimmel, 1994). The crest cells destined to populate the mandibular, hyoid and the 1st gill arch migrate in the vicinity of the otic placode (Schilling and Kimmel, 1994). Inappropriate positional information in the otic placode and possibly the surrounding tissues may result in misguided migration of neural crest cells and consequently in defective morphogenesis of the branchial arches. In another scenario, defects of the otic placode and misdirected migration of the neural crest could be a consequence of inappropriate hindbrain patterning. Expression patterns of *krox-20*, *pax-2* and *hlx-1* in *quo*^{m271} mutants suggest however that the overall brain pattern in this mutant is normal (this work and Neuhauss et al., 1996).

Lack of proper otolith formation in group III mutants (Table 1) may have diverse causes. One possibility is absence or abnormal development of the sensory epithelium which participates in otolith deposition. Another possible cause could be a biochemical defect preventing the uptake or deposition of organic or inorganic materials necessary for otolith formation. Lack of properly formed otoliths has been observed in several mouse mutants, for example: *pallid* (*pa*), *muted* (*mu*), *tilted head* (*thd*), and *lethal milk* (*lm*) (Green, 1990). Some of them have been characterized in detail. The pallid and muted phenotypes resemble a group of human diseases known as platelet storage pool deficiencies (Novak et al., 1984). In addition to the otolith phenotype, mutations in these loci produce changes in the subcellular structure of platelets, melanocytes and kidney cells. *pallid* has been recently shown to affect the

structure and expression of the gene encoding protein 4.2, a major component of the erythrocyte membrane (White et al., 1992).

Several limitations apply to our genetic analysis of ear development. Loci involved in ear morphogenesis may not have been identified as such due to their pleiotropic function during early embryonic development. This consideration is particularly relevant to relatively late developmental events, for example, morphogenesis of semicircular canals. The function of other loci may not have been revealed due to genetic redundancy. The design of our screen precluded isolation of fully penetrant dominant phenotypes involving lethality or maternal effect loci. Only one allele was recovered for more than half of the complemented loci (Table 1) indicating that many genes involved in the ear development remain unidentified.

Several features of the zebrafish embryo will facilitate effective phenotypic and genetic analysis of identified mutants. A number of sophisticated embryological manipulations are possible in zebrafish. Mosaic animals are easily generated by blastomere transplantations (Ho and Kane, 1990). Individual cells can be labeled and their fate followed in living embryos (Kimmel and Warga, 1986; Schilling and Kimmel, 1994) Heterotopic and heterochronic transplantations are possible at various stages of development (Eisen, 1991; Ho and Kimmel, 1993). These experimental tools will enable a detailed analysis of the mutant phenotypes identified in our screen. One would like to know for example whether the abnormal ear size and shape in *golas* and several other mutants is an intrinsic property of the otic vesicle or results from abnormal interactions with the surrounding tissues. This question can be efficiently addressed by otic placode transplantations. Similarly, it would be interesting to trace the pattern of neural crest migration in the mutant *quadro*^{m271}. Molecular characterization of the affected genetic loci is an obvious step in the future analysis of the identified mutations. Identification of candidate genes and if this is not possible, positional cloning will lead towards this goal. The first maps of the zebrafish genome are already available (Postlethwait et al., 1994; Knapik et al., 1996) and raise hopes for quick progress in this area.

We thank Colleen Boggs, Jane Belak, Ioannis Batjakas, Heather Goldsboro, Lisa Anderson, Snorri Gunnarson and Pamela Cohen for technical help during the various stages of the screen. We are also grateful to Julian Lewis, Tanya Whitfield and Catherine Haddon for sharing unpublished results and Eliza Mountcastle-Shah for critical reading of the manuscript. This work was supported in part by NIH RO1-HD29761 and a sponsored research agreement with Bristol Myers-Squibb (to W. D.). Further support in form of fellowships came from HFSP and the Fullbright Program (to Z. R.), EMBO and Swiss National Fond (to A. S.), Helen Hay Whitney Foundation (to D. L. S. and D. Y. S.), and the Damon Runyon - Walter Winchell Cancer Research Fund (to J. M.).

Note added in proof

Mutations in the genes *colourless* (Kelsh et al., 1996) and *golas* (this paper) fail to complement each other and thus are to be considered allelic. Future references to this gene should use the name *colourless*.

REFERENCES

Chakrabarti, D., Streisinger, J., Singer, F. and Walker, C. (1983). Frequency of gamma-ray induced specific locus and recessive lethal mutations in mature germ cells of the zebrafish, Brachydanio rerio. *Genetics* **103**, 109-123.

Chisaka, O., Musci, T. and Capecchi, M. (1992). Developmental defects of the ear, cranial nerves and hindbrain resulting from targeted disruption of the mouse homeobox gene Hox-1.6. *Nature* **355**, 516-520.

Chranilov, W. (1927). Beiträge zur Kenntniss des Weber'schen Apparates der Ostariophysi. 1. Vergleichend-anatomische Übersicht der Knochenelemente des Weber'schen Apparates bei Cypriniformes. *Zool. Jahrbücher (Anat.)* **49**, 501-597.

Cordes, S. and Barsh, G. (1994). The mouse segmentation gene kr encodes a novel basic domain-leucine zipper transcription factor. *Cell* **79**, 1025-1034.

Deol, M. (1964). The abnormalities of the inner ear in kreisler mice. *J. Embryol. exp. Morph.* **12**, 475-490.

Deol, M. (1968). Inherited diseases of the inner ear in man in the light of studies on the mouse. *J. Med. Genet.* **5**, 137-154.

Deol, M. (1970). The relationship between abnormalities of pigmentation and of the inner ear. *Proc. R. Soc. Lond. Biol.* **175**, 201-217.

Deol, M. (1980). Genetic malformations of the inner ear in the mouse and man. In *Morphogenesis and Malformation of the Ear.* (ed. Gorlin, R.), pp. 243-261. New York: Alan R. Liss, Inc.

Detwiler, S. and Van Dyke, R. (1950). The role of the medulla in the differentiation of the otic vesicle. *J. Exp. Zool.* **113**, 179-194.

Detwiler, S. and Van Dyke, R. (1951). Recent experiments on the differentiation of the labyrinth in Amblystoma. *J. Exp. Zool.* **118**, 389-401.

Driever, W., Solnica-Krezel, L., Schier, A. F., Neuhauss, S. C. F., Malicki, J., Stemple, D. L., Stainier, D. Y. R., Zwartkruis, F., Abdelilah, S., Rangini, Z., Belak, J. and Boggs, C. (1996). A genetic screen for mutations affecting embryogenesis in zebrafish. *Development* **123**, 37-46.

Eisen, J. S. (1991). Determination of primary motoneuron identity in developing zebrafish embryos. *Science* **252**, 569-572.

Ekker, M., Akimenko, M., Bremiller, R. and Westerfield, M. (1992). Regional expression of three homeobox transcripts in the inner ear of zebrafish embryos. *Neuron* **9**, 27-35.

Epstein, D., Vekemans, M. and Gros, P. (1991). splotch (Sp^{2H}), a mutation affecting development of the mouse neural tube, shows a deletion within the paired homeodomain of Pax-3. *Cell* **67**, 767-774.

Frohman, M., Martin, G., Cordes, S., Halamak, L. and Barsh, G. (1993). Altered rhombomere-specific gene expression and hyoid bone differentiation in the mouse segmentation mutant, kreisler (kr). *Development* **117**, 925-936.

Green, M. (1990). Catalog of mutant genes and polymorphic loci. In *Genetic Variants and Strains of the Laboratory Mouse* (ed. Lyon, M. and A. Searle), pp. 12-403. New York: Oxford University Press.

Haddon, C. and Lewis, J. (1996). Early ear development in the embryo of the zebrafish, Danio rerio. *J. Comp. Neurol.* **365**, 113-128.

Hawkins, A. and Horner, K. (1981). The acustico-lateralis system of aquatic vertebrates. In *Sense Organs* (ed. Laverack, M. and D. Cosens), pp. 220-254. Edinburgh: Blackie.

Ho, R. and Kane, D. (1990). Cell-autonomous action of zebrafish spt-1 mutation in specific mesodermal precursors. *Nature* **348**, 728-730.

Ho, R. and Kimmel, C. (1993). Commitment of cell fate in the early zebrafish embryo. *Science* **261**, 109-111.

Kimmel, C., Ballard, W., Kimmel, S., Ullmann, K. and Schilling, T. (1995). Stages of embryonic development of the zebrafish. *Dev. Dyn.* **203**, 253-310.

Kimmel, C. and Warga, R. (1986). Tissue-specific cell lineages originate in the gastrula of the zebrafish. *Science* **231**, 365-368.

Knapik, E. W., Goodman, A., Atkinson, O. S., Roberts, C. T., Shiozawa, M., Sim, C. U., Weksler-Zangen, S., Trolliet, M. R., Futrell, C., Innes, B. A., Koike, G., McLaughlin, M. G., Pierre, L., Simon, J. S., Vilallonga, E., Roy, M., Chiang, P.-W., Fishman, M. C., Driever, W. and Jacob, H. J. (1996). A reference cross DNA panel for zebrafish (*Danio rerio*) anchored with simple sequence length polymorphisms. *Development* **123**, 451-460.

Krauss, S., Johansen, T., Korzh, V., Moens, U., Ericson, J. and Fjose, A. (1991). Zebrafish pax[zf-a]: a paired box-containing gene expressed in the neural tube. *EMBO J.* **10**, 3609-3619.

Langille, R. and Hall, B. (1988). Role of the neural crest in development of the cartilaginous cranial and visceral skeleton of the medaka, *Oryzias latipes* (Teleostei). *Anat. Embryol.* **177**, 297-305.

Le Lievre, C. (1978). Participation of neural crest-derived cells in the genesis of the skull in birds. *J. Embryol. exp. Morph.* **47**, 17-37.

Lim, D. (1980). Morphogenesis and malformation of otoconia: a review. In *Morphogenesis and Malformation of the Ear.* (ed. Gorlin, R.), pp. 111-146. New York: Alan R. Liss, Inc.

Malicki, J., Neuhauss, S. C. F., Schier, A. F., Solnica-Krezel, L., Stemple, D. L., Stainier, D. Y. R., Abdelilah, S., Zwartkruis, F., Rangini, Z. and Driever, W. (1996). Mutations affecting development of the zebrafish retina. *Development* **123**, 263-273.

Mansour, S., Goddard, J. and Capecchi, M. (1993). Mice homozygous for a targeted disruption of the proto-oncogene int-2 have developmental defects in the tail and inner ear. *Development* **117**, 13-28.

Mullins, M., Hammerschmidt, M., Haffter, P. and Nusslein-Volhard, C. (1994). Large-scale mutagenesis in the zebrafish: in search of genes controlling development in vertebrate. *Curr. Biol.* **4**, 189-202.

Neuhauss, S. C. F., Solnica-Krezel, L., Schier, A. F., Zwartkruis, F., Stemple, D. L., Malicki, J., Abdelilah, S., Stainier, D. Y. R. and Driever, W. (1996). Mutations affecting craniofacial development in zebrafish. *Development* **123**, 357-367.

Noden, D. (1983). The role of the neural crest in patterning of avian cranial skeletal, connective and muscle tissues. *Dev. Biol.* **96**, 144-165.

Novak, E., Hui, S. and Swank, R. (1984). Platelet storage pool deficiency in mouse pigment mutations associated with seven distinct genetic loci. *Blood* **63**, 536-544.

Oxtoby, E. and Jowett, T. (1993). Cloning of the zebrafish krox-20 gene (krx-20) and its expression during hindbrain development. *Nucl. Acids Res.* **21**, 1087-1095.

Pavan, W. and Tilghman, S. (1994). Piebald lethal (s^l) acts early to disrupt the development of neural crest-derived melanocytes. *Proc. Natl. Acad. Sci. USA* **91**, 7159-7163.

Platt, C. (1993). Zebrafish inner ear sensory surfaces are similar to those in goldfish. *Hearing Research* **65**, 133-140.

Popper, A. and Fay, R. (1993). Sound detection and processing by fish: critical review and major research questiones. *Brain Behav. Evol.* **41**, 14-38.

Postlethwait, J. H., Johnson, S. L., Midson, C. N., Talbot, W. S., Gates, M., Ballinger, E. W., Africa, D., Andrews, R., Carl, T., Eisen, J. S. and et al. (1994). A genetic linkage map for the zebrafish. *Science* **264**, 699-703.

Retzius, G. (1881). *Das Gehörorgan der Wirbelthiere. Morphologisch-histologische Studien.* vol. 1. Stockholm: Samson and Wallin.

Retzius, G. (1884). *Das Gehörorgan der Wirbelthiere. Morphologisch-histologische Studien.* vol. 2. Stockholm: Samson and Wallin.

Schier, A. F., Neuhauss, S. C. F., Harvey, M., Malicki, J., Solnica-Krezel, L., Stainier, D. Y. R., Zwartkruis, F., Abdelilah, S., Stemple, D. L., Rangini, Z., Yang, H. and Driever, W. (1996). Mutations affecting the development of the embryonic zebrafish brain. *Development* **123**, 165-178.

Schilling, T. and Kimmel, C. (1994). Segment and cell type lineage restrictions during pharyngeal arch development in the zebrafish embryo. *Development* **120**, 483-494.

Solnica-Krezel, L., Schier, A. and Driever, W. (1994). Efficient recovery of ENU-induced mutations from the zebrafish germline. *Genetics* **136**, 1-20.

Stainier, D. Y. R., Fouquet, B., Chen, J.-N., Warren, K. S., Weinstein, B. M., Meiler, S., Mohideen, M.-A. P. K., Neuhauss, S. C. F., Solnica-Krezel, L., Schier, A. F., Zwartkruis, F., Stemple, D. L., Malicki, J., Driever, W. and Fishman, M. C. (1996). Mutations affecting the formation and function of the cardiovascular system in the zebrafish embryo. *Development* **123**, 285-292.

Steel, K. P. and Brown, S. D. (1994). Genes and deafness. *Trends Genet.* **10**, 428-35.

Waterman, R. and Bell, D. (1984). Epithelial fusion during early semicircular canal formation in the embryonic zebrafish, Brachydanio rerio. *Anat. Rec.* **210**, 101-114.

Westerfield, M. (1994). *The Zebrafish Book.* Eugene: University of Oregon Press.

White, R., Peters, L., Adkison, L., Korsgren, C., Cohen, C. and Lux, S. (1992). The murine pallid mutation is a platelet storage pool disease associated with the protein 4.2 (pallidin) gene. *Nature Genetics* **2**, 80-83.

(Accepted 16 November 1995)